Paleoceanography and Paleoclimatology

RESEARCH ARTICLE
10.1029/2017PA003290

Key Points:
- Deglacial ocean circulation changes were recorded with εNd in high resolution at the abyssal Corner Rise
- Distinct contribution of Northern Component Water is detectable at the abyssal northwest Atlantic during the Last Glacial Maximum
- The $\delta^{13}C$ and εNd are partly decoupled at Corner Rise, implying nonconservative behavior of one or both proxies

Supporting Information:
- Supporting Information S1

Correspondence to:
F. Pöppelmeier,
frerk.poeppelmeier@geow.uni-heidelberg.de

Citation:
Pöppelmeier, F., Gutjahr, M., Blaser, P., Keigwin, L. D., & Lippold, J. (2018). Origin of abyssal NW Atlantic water masses since the Last Glacial Maximum. *Paleoceanography and Paleoclimatology*, *33*, 530–543. https://doi.org/10.1029/2017PA003290

Received 14 NOV 2017
Accepted 22 APR 2018
Accepted article online 7 MAY 2018
Published online 31 MAY 2018

Origin of Abyssal NW Atlantic Water Masses Since the Last Glacial Maximum

F. Pöppelmeier[1], M. Gutjahr[2], P. Blaser[1], L. D. Keigwin[3], and J. Lippold[1]

[1]Institute of Earth Sciences, Heidelberg University, Heidelberg, Germany, [2]GEOMAR Helmholtz Centre for Ocean Research Kiel, Kiel, Germany, [3]Department of Geology and Geophysics, Woods Hole Oceanographic Institution, Woods Hole, MA, USA

Abstract The notion of a shallow northern sourced intermediate water mass is a well evidenced feature of the Atlantic circulation scheme of the Last Glacial Maximum (LGM). However, recent observations from stable carbon isotopes ($\delta^{13}C$) at the Corner Rise in the deep northwest Atlantic suggested a significant contribution of a Northern Component Water mass to the abyssal northwest Atlantic basin that has not been described before. Here we test the hypothesis of this northern sourced water mass underlying the southern sourced glacial Antarctic Bottom Water by measuring the authigenic neodymium (Nd) isotopic composition from the same sediments from 5,010-m water depth. Neodymium isotopes act as a semiconservative water mass tracer capable of distinguishing between Northern and Southern Component Waters at the northwest Atlantic. Our new Nd isotopic record resolves various water mass changes from the LGM to the early Holocene in agreement with existing Nd-based reconstructions from across the west Atlantic Ocean. Especially pronounced are the Younger Dryas and Bølling-Allerød with unprecedented changes in the Nd isotopic composition. For the LGM we found Nd isotopic evidence for a northern sourced water mass contributing to abyssal depths, thus being in agreement with previous $\delta^{13}C$ data from Corner Rise. Overall, however, the deep northwest Atlantic was still dominated by southern sourced water, since we found signatures that are intermediate between northern and southern end member compositions. Furthermore, this new record indicates that C and Nd isotopes were partly decoupled, pointing to nonconservative behavior of one or more likely of both water mass proxies during the LGM.

1. Introduction

The main features and reorganizations of Atlantic Meridional Overturning Circulation (AMOC) modes are moderately well understood for the past 25,000 years (Curry & Oppo, 2005; Lippold et al., 2016; McManus et al., 2004; Roberts et al., 2010). However, the exact distribution and propagation of participating water masses during key (de)glacial intervals is less well resolved. The modern deep water circulation in the North Atlantic is characterized by two main constituents. In the Nordic Seas and the Labrador Sea deep convection produces dense water masses flowing southward, mixing and thereby forming North Atlantic Deep Water (NADW). Its southern counterpart, Antarctic Bottom Water (AABW), is denser and occupies most of the deep southwestern Atlantic but can be identified in the abyssal North Atlantic even up to 45°N (Schmitz, 1996). Compared to the modern configuration, the Atlantic water mass distribution and circulation was vastly different during the Last Glacial Maximum (LGM) and Heinrich ice rafting events HE2 and HE1 (e.g., Roberts et al., 2010; Sarnthein et al., 1994). Sea ice cover and stratification shifted the area of northern deep water formation southward (Duplessy et al., 1980). Furthermore, a shoaled NADW circulation cell, often referred to as Glacial North Atlantic Intermediate Water (Boyle & Keigwin, 1987), was accompanied by an enhanced northward penetration of Southern Component Water (SCW) below (e.g., Adkins, 2013). On the other hand, Keigwin and Swift (2017) recently presented radiocarbon as well as stable carbon isotopic data suggesting the presence of northern sourced water in the abyssal (below 4,500-m water depth) NW Atlantic basin into glacial SCW during the LGM admixed. The presence of deep glacial Northern Component Water (NCW) in the abyssal North Atlantic was also indirectly inferred from a compilation of neodymium (Nd) isotope data from sediment cores that were shallower than the one used by Keigwin and Swift (2017) and this study (Howe, Piotrowski, Noble, et al., 2016). The latter study, however, proposed that NCW was admixed into SCW below 2,500-m water depth, leading to a decreasing contribution of NCW with depth.

In order to critically evaluate the suggested presence of the enigmatic abyssal NCW during the LGM, we present a high-resolution Nd isotope record from Corner Rise (CR) core KNR197/10 GGC17 (36°24.3′N, 48°32.4′W)

10.1029/2017PA003290

from the deep NW Atlantic (5,010 m), extracted from authigenic sedimentary Fe-Mn oxyhydroxides. Owing to its position, this site is sensitive to track the existence of the proposed Glacial Northwest Atlantic Bottom Water. In combination with its average to high sedimentation rates (5–10 up to 40 cm/kyear during the Younger Dryas, YD, period) as well as surprisingly good preservation of foraminifera (Keigwin & Swift, 2017) this location is perfectly suited for abyssal bottom water mass reconstructions. Comparison of Nd isotopes with recent δ^{13}C and Δ^{14}C from the very same core (Keigwin & Swift, 2017) allows us an improved assessment of the origin and mixing proportion of the local bottom water masses, and the potentially variable degree of remineralization at the core site. Given that the same sediment material is used here, any chronological issues and offsets between the δ^{13}C record by Keigwin and Swift (2017) and the new Nd isotope record can be excluded.

1.1. Nd Isotopes as a Proxy for Water Mass Provenance

Even though the stable carbon isotope composition (δ^{13}C) of seawater and benthic foraminifera is a well-established and commonly used paleoceanographic proxy (e.g., Curry & Oppo, 2005; Sarnthein et al., 1994), effects such as remineralization, air-sea gas exchange, or changes in the export productivity can complicate the interpretation of these data. For instance, an increase in export productivity or a more sluggish AMOC have the potential to decrease the ambient deep water dissolved δ^{13}C significantly and therefore need to be considered carefully in evaluating δ^{13}C data (Gebbie, 2014). In comparison, the neodymium isotope proxy is independent of biological and gas exchange processes (Frank, 2002; Goldstein & Hemming, 2003; Vance et al., 2004). However, the mostly unknown mechanisms, magnitude and geographic variability of boundary exchange, a process where Nd is exchanged between particulate and dissolved phases along continental margins (Jeandel, 2016; Lacan & Jeandel, 2005a) and mismatches between filtered and unfiltered seawater data (e.g., Lambelet et al., 2016, versus Piepgras & Wasserburg, 1987), make the interpretation of Nd isotope signatures similarly challenging as stable carbon isotope data. The combination of these two proxies, however, presents a well-suited approach to unravel marine carbon cycle-related processes and boundary exchange from changes in water mass provenance.

In the deep Atlantic, Nd has an oceanic residence time of 350–500 years and is thus considered a quasi-conservative tracer of water masses (Tachikawa et al., 2003). The main sources of dissolved Nd to the oceans are riverine continental input and boundary exchange along the margins (Frank, 2002; Lacan & Jeandel, 2005a; Rempfer et al., 2011). Highly diverse crustal formation ages (Archean formations in North America versus young rocks on Iceland) result in a large range of circum-North Atlantic Nd isotopic signatures. This feature produces well resolvable differences in εNd values (relative deviation of the sample ^{143}Nd/^{144}Nd ratio normalized to the *Chondritic Uniform Reservoir* in parts per ten thousand) of all involved modern water masses, allowing the identification of mixing processes and water mass provenance (Lacan & Jeandel, 2005b; Lambelet et al., 2016). The northern NADW can be divided into three layers, namely, upper, middle, and lower NADW with different source regions. Due to the relevance to this study only lower NADW (or Northwest Atlantic Bottom Water, NWABW) will be described (Figure 1). Its main contribution comes from Denmark Strait Overflow Water, which is the densest water mass formed in the North Atlantic today. In terms of εNd this water mass is rather radiogenic with a modern end member of around εNd = -8.4 ± 1.4 (Lacan & Jeandel, 2004). Mixing with unradiogenic Labrador Sea Water (LSW; εNd = -14.2 ± 0.3, Lambelet et al., 2016) and Subpolar Mode Water (-13 to -15, Lacan & Jeandel, 2004) it forms NWABW in the subpolar North Atlantic. At around 50°N and 30°N, western Lower Deep Water (originated from modified AABW, εNd = -12.5 ± 0.4, Lacan & Jeandel, 2005b) further contributes to NWABW (Schmitz, 1996). Due to the mixing of these various water masses, NWABW gradually changes its isotopic composition from around -11 southeast of Greenland to -12.4 after leaving the Labrador Sea (Lacan & Jeandel, 2005b; Lambelet et al., 2016). Further, boundary exchange possibly contributes to this εNd shift of NWABW in the Labrador Sea (Lacan & Jeandel, 2005a; van de Flierdt et al., 2016).

The main constituent of SCW is AABW, which is characterized by low temperatures, high nutrient concentrations and low salinity (Rijkenberg et al., 2014). Its present-day Southern Ocean εNd value of about -8.5 is modified on its northward flow and detectable up to 45°N where modified AABW exhibits an εNd value of -12.2 after mixing continuously with the more unradiogenic overlaying NADW (Lambelet et al., 2016). In terms of water masses, site KNR197/10 is currently situated near the interface between modified AABW and NWABW (Schmitz, 1996).

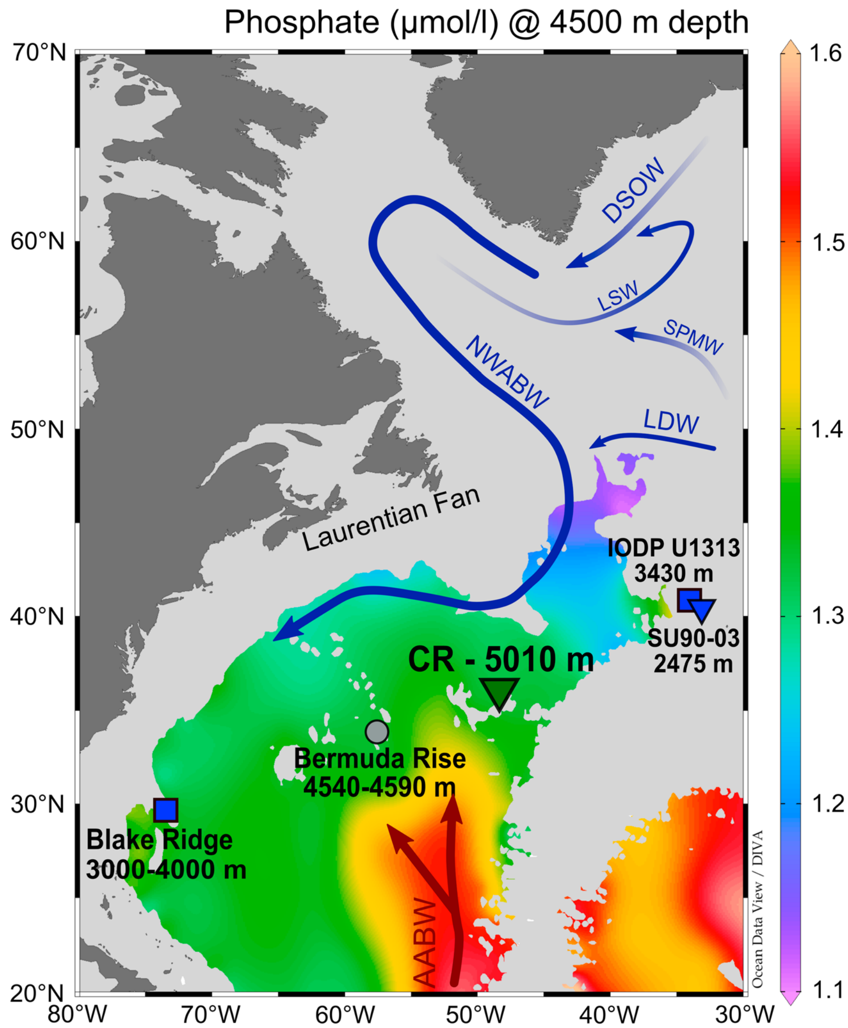

Figure 1. Map of phosphate concentration at 4,500-m water depth (World Ocean Atlas 2013; Garcia et al., 2014) with modern deep water currents (northern sourced water masses in blue and southern sourced in red). NWABW forms by combining Subpolar Mode Water, LSW, and DSOW (depleted in phosphate). It is further modified by Lower Deep Water at 50°N (Schmitz, 1996). AABW enters the NW Atlantic basin from the south (enriched in phosphate). Core locations at CR (KNR197/10 GGC17, 36°24′N, 48°32′W, 5,010 m, this study), Bermuda Rise (ODP 1063, 33°41′N, 57°37′W, 4,584 m, Böhm et al., 2015; Gutjahr & Lippold, 2011; OCE326-GGC5, 33°42′N, 57°35′W, 4,550 m, McManus et al., 2004; OCE326-GGC6, 33°41′N, 57°35′W, 4,541 m, Roberts et al., 2010), Blake Ridge (ODP 1059–1061, ~30°N, ~74°W, 3,000–4,000 m, this study), IODP U1313 (41°00′N, 32°58′W, Lippold et al., 2016), and SU90-03 (40°05′N, 32°00′W, Howe, Piotrowski, Noble, et al., 2016) are depicted as green triangle, gray circle, and blue squares/triangle, respectively. DSOW = Denmark Strait Overflow Water; LSW = Labrador Sea Water; NWABW = North West Atlantic Bottom Water; AABW = Antarctic Bottom Water; CR = Corner Rise.

2. Materials and Methods

2.1. Sediment Cores

Sediment core KNR197/10 GGC17 (36°24.3′N, 48°32.4′W) was retrieved from the CR in the deep northwest Atlantic from a water depth of 5,010 m (Figure 1). The general sediment composition is described in Keigwin and Swift (2017) and consists mainly of greenish clay with nannofossil beds. Core chronology was established via 11 AMS ^{14}C datings (corrected with a constant 400 year reservoir age) on the planktonic foraminifera *Globorotalia inflata* with linear interpolation assuming the core top to be zero age (Keigwin & Swift, 2017) covering the last 25 ka. Sedimentation rates range from 5 to 10 cm/ka in the Holocene and LGM sections and up to 40 and 23 cm/ka during the YD and late glacial, respectively (Figure 2d). XRD and magnetic susceptibility measurements were performed on GGC17 to investigate the mineralogic composition (Figures S1–S3 in the supporting information). Furthermore, three sediment cores from Blake Ridge (31°N,

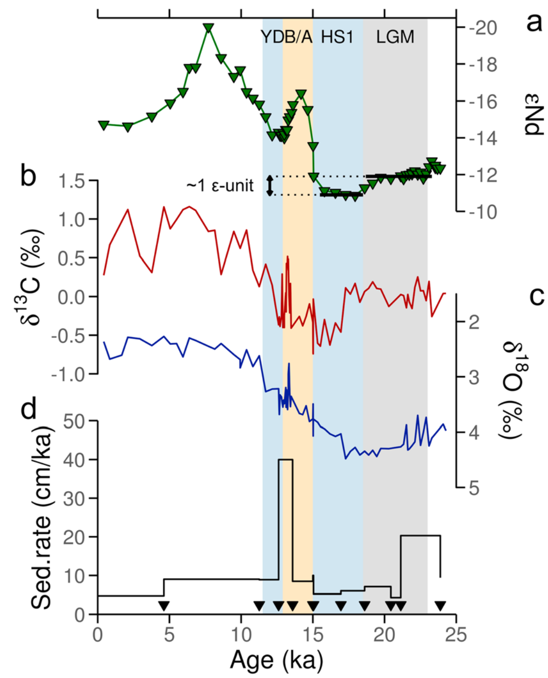

Figure 2. Corner Rise (KNR197/10 GGC17) data covering the past 25 ka by Keigwin and Swift (2017) and this study: (a) εNd record extracted from authigenic sedimentary phases from this study. Shift of 1 ε from LGM to HS1 is indicated by dashed lines (see section 3.2). The 2σ external uncertainty is smaller than symbol size. (b and c) Benthic δ^{13}C and δ^{18}O data from same core published by Keigwin and Swift (2017). (d) Sedimentation rate in centimeters per kiloannum. Black triangles at the bottom panel depict the ^{14}C age tie points by Keigwin and Swift (2017). Note the reversed scale for εNd. Vertical bars indicate the time ranges of the LGM, HS1, B/A, and YD. LGM = Last Glacial Maximum; B/A = Bølling-Allerød; YD = Younger Dryas.

75°W; Grützner et al., 2002) forming a depth transect and IODP Site U1313 (Lippold et al., 2016; Naafs et al., 2013) were sampled for the LGM and deglacial, respectively (Figure 1 and detailed description in Table S1).

In addition, δ^{13}C of *Cibicidoides* is reported here from core Atlantis II (AII) 107 22GGC (54°48′S, 03°20′W, 2,768 m) from the LGM section for an improved glacial SCW end member δ^{13}C estimation (Table S2; Keigwin & Boyle, 1989).

2.2. Analytical Procedures

The past bottom water Nd isotopic composition can be recovered from biogenic material (Palmer, 1985; Roberts et al., 2010; van de Flierdt et al., 2010) or from authigenic sedimentary phases (Blaser et al., 2016; Frank, 2002; Piotrowski et al., 2012; Wilson et al., 2013). In the latter case, Nd is incorporated into authigenic Fe-Mn oxyhydroxides precipitated onto particles at the sediment-water interface, preserving the bottom water Nd isotopic signature (Haley et al., 2004). Here the extraction of the authigenic Nd fraction of the bulk sediment was carried out following the procedure of Blaser et al. (2016). Dried and ground sediment was leached at room temperature for about 1 hr with 0.005 M hydroxylamine hydrochloride—0.003 M EDTA—1.5% (*v*/*v*) acetic acid—0.1% (v/v) ammonia (for buffering to pH = 4) in a shaker. After centrifugation, the supernatant was transferred to Teflon vials and further processed by a two-step column chromatography following the protocols of Cohen et al. (1988) and Pin et al. (1994). Blaser et al. (2016) have shown that leaching with such a weak acid-reductive solution is well suited for northern Atlantic sediments and the extracted signal is dominated by the authigenic phases. The same study also showed that this weak leaching method reproduced the Nd isotopic composition of foraminifera even where foraminifera themselves were offset from seawater data. Furthermore, Böhm et al. (2015) reproduced leachate data with foraminifera at Nd isotope peaks as unradiogenic as −18 at the nearby Bermuda Rise, indicating that the leaching method extracts a pore water or bottom water Nd isotopic signature, not significantly influenced by the detrital fraction. The only difference to the method proposed by Blaser et al. (2016) was buffering of the leachate with a 0.1% (v/v) ammonia solution (supra pure) instead of NaOH, originally introduced by Gutjahr et al. (2007), to avoid the introduction of excess Na to the leachate in order to simplify element concentration measurements.

Neodymium isotopes were measured on a Neptune Plus MC-ICP-MS at GEOMAR Helmholtz Centre for Ocean Research Kiel. Machine-induced mass fractionation was corrected for internally by an exponential law normalizing the raw data to ^{146}Nd/^{144}Nd = 0.7219. Samples were further bracketed by JNdi-1 standard solutions with Nd isotopic compositions normalized to the accepted value of 0.512115 (Tanaka et al., 2000). A secondary standard solution measured in sequence with identical concentration of ~50 ppb Nd in solution reproduced at −3.72 ± 0.15 εNd (*n* = 14, 2 SD). As expected, the 2 sigma external reproducibility of 0.15 ε slightly exceeded the 2 SE internal uncertainty for all samples (Table S3). Total procedural blanks were below 83 pg and hence negligible.

3. Results and Discussion

Corner Rise Nd isotopic compositions extracted from authigenic Fe-Mn oxyhydroxides of bulk sediment are shown in Figure 2 in comparison with the stable carbon and oxygen isotope data from the same core (Keigwin & Swift, 2017). During the LGM εNd values slowly increased from −12.5 to −11.6, with an average value of about −12.0. The most radiogenic εNd values were recorded during HS1 (−10.9) and are roughly 1 ε more radiogenic than the LGM values. From 5 to 15 ka the CR data clearly delineate well-defined millennial-scale changes, especially during the Bølling-Allerød (B/A), YD, and the early Holocene. In detail, the Nd isotopic compositions drop by about 5 ε during the transition from HS1 (−10.9) to the B/A (−16.4) in striking agreement with oxygen isotopic changes seen in Greenland ice cores (Figure 3). The cold YD

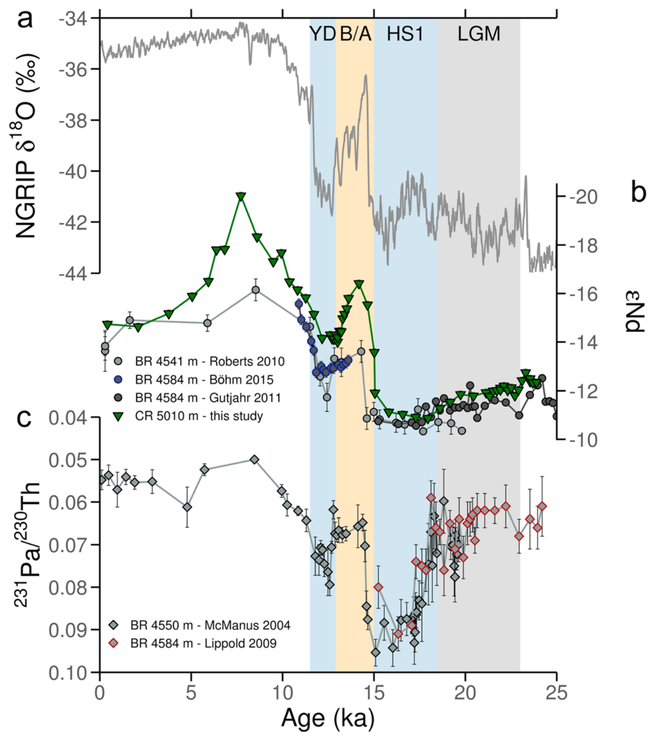

Figure 3. (a) Oxygen isotope record of the NGRIP ice core (NGRIP Members, 2004; b) Comparison of εNd data from Bermuda Rise (Böhm et al., 2015; Gutjahr & Lippold, 2011; Roberts et al., 2010) and Corner Rise (this study) over the past 25 ka. The 2σ uncertainties are shown but are smaller than symbol size for the data of Gutjahr and Lippold (2011) and this study. (c) $^{231}Pa/^{230}Th$ data from Bermuda Rise (Lippold et al., 2009; McManus et al., 2004). Larger values indicate reduced AMOC strength and smaller values a more vigorous circulation. Note the reversed scales for εNd and $^{231}Pa/^{230}Th$. Vertical bars indicate the time ranges of the LGM, HS1, B/A, and YD. AMOC = Atlantic Meridional Overturning Circulation; LGM = Last Glacial Maximum; B/A = Bølling-Allerød; YD = Younger Dryas.

period was again dominated by more radiogenic εNd values around −14. During the Holocene εNd dropped again, but this time to values as unradiogenic as −20. This early Holocene "overshoot" is a common feature in the northwest Atlantic sedimentary records (e.g., Gutjahr et al., 2008; Lippold et al., 2016; Roberts et al., 2010) but has not been reported before with such a large amplitude of ΔεNd = −9 (compared to HS1).

3.1. NW Atlantic Authigenic εNd

Comparison of the CR core top εNd value (−14.7 ± 0.2, Figure 2) to proximate seawater data from Piepgras and Wasserburg (1987; −13.6 ± 0.3) and Lambelet et al. (2016; −12.7 ± 0.2) shows a discrepancy of about 1 and 2 ε-units, respectively. The difference between these two earlier seawater studies could be accounted for by the fact that Piepgras and Wasserburg (1987) measured unfiltered seawater, while Lambelet et al. (2016) used filtered seawater. Thus, a reactive particulate phase ultimately derived from the Northeast American continent or West Greenland (εNd = −25 to −35; Jeandel et al., 2007) could have influenced the unfiltered seawater data. This hypothetical process would have further implications on the sedimentary phase, since this material possibly continued to react with pore fluids after deposition, exchanging its Nd with the authigenic phase (Abbott et al., 2016). Pore water Nd, partly derived from detrital material, influencing the authigenic phase at the sediment-bottom water interface was also recently observed by Du et al. (2016) in the Gulf of Alaska. Since this process is proposed to be dependent on the benthic exposure time, sediments from the well-ventilated Atlantic should be less influenced by this. Nevertheless, such a benthic exchange process is a valid mechanism to produce an offset between core top and seawater signatures at CR and thus presents a potential explanation. This process could also explain a similar offset between the filtered seawater data from Lambelet et al. (2016) and the core top data at Bermuda Rise (Roberts et al., 2010). In this context, Howe, Piotrowski, and Rennie (2016) recently argued for an abyssal origin of unradiogenic εNd in the NW Atlantic during the early Holocene, sourced from poorly weathered material deposited into the Labrador Sea (εNd = −25 to −20; Fagel et al., 1999), which temporarily released its unradiogenic signature to bottom waters that were subsequently advected into the open NW Atlantic. The offset between nearby seawater and authigenic Nd isotope data at CR could equally be explained by such a process. Since the leaching approach is very gentle (Blaser et al., 2016) we consider the possibility of leaching artifacts (such as a dominant contribution of leached detrital Nd; e.g., Wilson et al., 2013) as highly unlikely. Besides, previous studies presenting clear evidence for leaching artifacts in this region were commonly associated with more radiogenic εNd signatures than ambient bottom water, not less such as observed here (Blaser et al., 2016; Elmore et al., 2015; Roberts et al., 2010; although unradiogenic imprints within the leachates from the Labrador Sea are possible; Blaser et al., 2016). However, the abovementioned processes potentially produce an offset that is significantly smaller than the difference in εNd between NADW and pure AABW.

The CR site is clearly recording Northern Hemispheric paleoclimatic and paleoceanographic overall structure and trends as well as showing clear analogies to previous deep NW Atlantic εNd records (Böhm et al., 2015; Gutjahr & Lippold, 2011; Roberts et al., 2010, and Figure 3). It is also noteworthy that if authigenic Nd isotopic compositions were modified in situ in parts of our record, then these extracted εNd were altered toward *less* radiogenic compositions, hence suggesting increased presence of NCW, while the glacial and early deglacial sections in our sediment core suggest the opposite.

In general, the CR record is consistently less radiogenic than the Bermuda Rise record (Figure 3), but in agreement with the abovementioned potential process of a reactive nepheloid layer of unradiogenic particles (Biscaye & Eittreim, 1977; Middag et al., 2015).

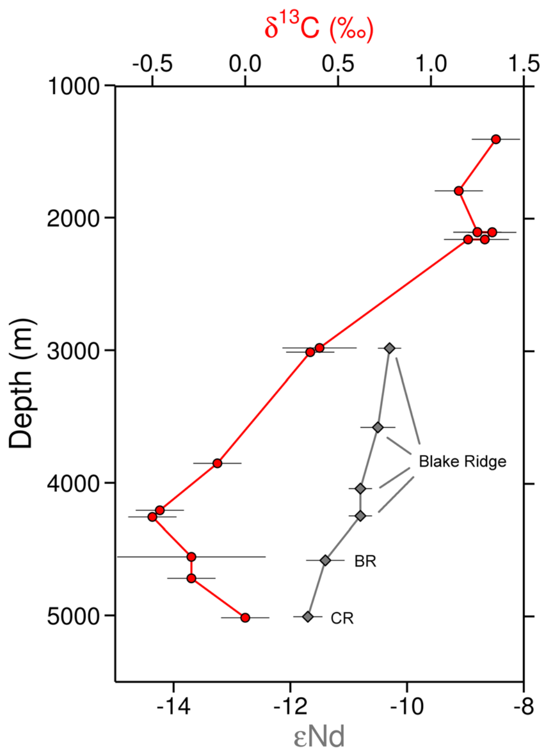

Figure 4. LGM depth transect of the NW Atlantic. $\delta^{13}C$ data are depicted in red (Keigwin, 2004; Keigwin & Boyle, 2008; Keigwin & Swift, 2017). Dark gray data show Bermuda Rise (Böhm et al., 2015; Gutjahr & Lippold, 2011; Roberts et al., 2010), Blake Ridge (Gutjahr et al., 2008, and ODP 1059, 1060, and 1061 from this study; see Tables S1 and S4 for description), and CR (this study). εNd values are LGM averages (18–22 ka) with 2 SD error bars. LGM = Last Glacial Maximum; CR = Corner Rise.

3.2. Abyssal Water Masses During the LGM in the NW Atlantic

In the deep NW Atlantic, εNd ranged between −10.2 and −11.4 during the LGM (Gutjahr et al., 2008; Gutjahr & Lippold, 2011; Howe, Piotrowski, & Rennie, 2016; Roberts et al., 2010). In terms of $\delta^{13}C$, modern NCW exhibits values of 1 to 1.3‰ while SCW is associated with lower values around 0.5‰ (Curry & Oppo, 2005). Keigwin and Swift (2017) found $\delta^{13}C$ at the CR elevated by about half a permil throughout the LGM compared to HS1 (Figure 2b). Such isotopic differences are comparable to those between modern ocean NADW and AABW. Further comparison to shallower NW Atlantic $\delta^{13}C$ records, forming a depth transect, revealed a reversal of the $\delta^{13}C$ trend below 4.2 km (see Figure 3a in Keigwin and Swift (2017) and Figure 4 of this study). Below this depth the data indicate increased admixtures of higher $\delta^{13}C$ water. Keigwin and Swift (2017) interpreted this as a contribution from a deep northern source. This suggestion is based on the observation that southern sourced water masses are today more depleted in ^{13}C. This holds most likely also for the LGM, even though the glacial southern end member is less well constrained than the northern one due to lack of data (Gebbie et al., 2015). ^{13}C gets further depleted by the long transit time of water masses from the south via the midlatitude North Atlantic being constantly replenished with remineralized organic matter through vertical water column supply (Gebbie, 2014). Keigwin and Swift (2017) further excluded the Nordic Seas as a source of this NCW since the newly discovered water mass contribution was reasonably well ventilated with somewhat elevated benthic radiocarbon contents, which is in contrast to recent findings that deep water of the Nordic Seas featured extremely high ^{14}C ages during the LGM (Thornalley et al., 2015). Thus, by process of elimination the Labrador Sea was identified as the only plausible origin of deep northern sourced water. Furthermore, Keigwin and Swift (2017) noted that an analogous feature was recorded by the GEOSECS mission in 1972, where NCW was detected at abyssal depth in the NW Atlantic, displacing the local modified AABW.

In the hydrographic setting of the LGM, εNd of NWABW should either have been as unradiogenic as today (−12.6, Lambelet et al., 2016) or possibly more unradiogenic due to increased influence from boundary exchange in the Labrador Sea, caused by a more sluggish deep circulation and thus longer residence times (Fagel et al., 1997, 1999; Jeandel, 2016). However, during the LGM the authigenic phase of the CR sediments recorded εNd values as radiogenic as −11.5. Since pure Labrador Sea sourced water should be clearly detectable by significantly less radiogenic values, as seen during the onset of the B/A (Figures 2 and 3), we exclude the possibility of a Labrador Sea sourced water mass dominating the abyssal NW Atlantic during the LGM. No continental source is known around the northern NW Atlantic possibly imprinting such radiogenic signatures into the water mass unless unrealistically high contributions of radiogenic Icelandic Nd contributed to the abyssal glacial NADW. In fact, the only deep water masses inheriting such radiogenic values today are the Nordic Seas overflow waters and southern AABW (−8.3 and −8.0, Lacan & Jeandel, 2004, and Lacan et al., 2012, respectively). In agreement with previous studies (Böhm et al., 2015; Lippold et al., 2016; Piotrowski et al., 2008; Roberts et al., 2010) we exclude the Nordic Seas as a source area for dense bottom water during the LGM. Taking into account the southward shifted and reduced deep water formation in the Greenland Sea during the LGM, Iceland Scotland Overflow Water (ISOW), and Denmark Strait Overflow Water may have been weakened and shoaled (Fagel et al., 2002; Millo et al., 2006). Two studies suggested persistent overflow from the GIN Seas during the LGM reporting water with relatively high εNd passing the Wyville-Thomson Ridge (Crocker et al., 2016; Crocket et al., 2010). However, if this water mass indeed descended deep enough in the subpolar North Atlantic moving as a deep boundary current analogous to today, it would first have passed through the Labrador Sea where it would have been admixed into less radiogenic deep waters. Thus, it is unlikely that the contribution of northern overflow waters was high enough to produce the Nd isotopic signal of −11.5 at CR. Therefore, the most probable source of more radiogenic Nd at CR during the LGM is the South Atlantic.

However, the Nd isotopic composition at CR during the LGM neither recorded the modern signature of the southern end member of around −8.5 (Goldstein & Hemming, 2003), nor the even more radiogenic glacial one of −6.5 (Basak et al., 2018; Skinner et al., 2013). Thus, an unradiogenic northern component is still required to get a value of −11.5. Howe, Piotrowski, Noble, et al. (2016) calculated the fractional contribution of glacial NADW at the proximate but shallower Bermuda Rise to be at least 42%. These authors inferred that a deep glacial NADW flux, albeit much smaller than modern, propagated southward into the deep NW Atlantic during the LGM. This scenario of NCW contributing to the abyssal NW Atlantic is, not in magnitude but in sense, in agreement with the $\delta^{13}C$ data of Keigwin and Swift (2017) and also the new εNd record of this study. However, whether this NCW contribution was rather confined to the deepest part of the basin or if it was admixed to the whole water column is difficult to distinguish with the current data set. The more radiogenic LGM data from Bermuda Rise and Blake Ridge (Gutjahr et al., 2008; Roberts et al., 2010; Figure 4) indicate the former, but this difference can, at least in part, also result from increased contributions of SCW bathing the more southern locations.

Further, the small but well-resolved increase of εNd during the transition from the LGM to HS1 at CR as well as at Bermuda Rise (Figures 2a and 3b, respectively) indicates a contribution from a northern sourced water mass during the LGM that is reduced during HS1. While nonconservative behavior could also explain this shift in εNd by the alteration of the authigenic Nd isotopic composition by pore water processes, two arguments can be used against it: First, the occurrence of the εNd shift at CR as well as Bermuda Rise hint to a nonlocal effect such as water mass advection. Second, Kurzweil et al. (2010) found (based on authigenic Pb isotopes) a constant weathering input signal of mature material at the Laurentian Fan during the transition from the LGM to HS1. In contrast, the Holocene was characterized by weathering of young, reactive material. Further, given that direct runoff and weathering input from NE American sources was significantly reduced (Kurzweil et al., 2010), likely a very similar situation persisted at the proximate CR. This is also indicated by the magnetic susceptibility at CR (Figure S1) which closely follows the weathering signal at the Laurentian Fan (Kurzweil et al., 2010) as well as the εNd signature at CR. This indicates a potentially significant weathering or pore water control on authigenic εNd during times of deep NADW convection. However, the lack of changes in the mineralogic composition (as seen from the XRD spectra; Figures S2 and S3) indicates a rather constant sediment provenance. From this we infer (if present at all) constant nonconservative effects for the LGM-HS1 transition. In addition, it is thought that during HS1 the northern deep water production was significantly weakened due to freshening of surface waters (Bradtmiller et al., 2014; McManus et al., 2004). Thus, the contribution of AABW in the NW Atlantic should have been more pronounced, leading to elevated εNd as seen in the new record (Figure 2a) and as seen as minimum $\delta^{13}C$ (Figure 2b) at CR.

3.3. Northern Sourced Contribution to the Abyssal NW Atlantic During the LGM

In order to estimate the contribution of northern sourced water to the abyssal NW Atlantic during the LGM a simple two end member calculation with binary mixing was performed. Since past seawater Nd concentrations can, at present, not be reconstructed, we assumed equal concentrations for both end members. This rough but reasonable assumption is based on modern water masses occupying similar depths also having similar Nd concentrations, for the reason that the Nd concentration is in first order a function of depth (cf. Lambelet et al., 2016; Stichel et al., 2012). During the LGM the southern εNd end member was determined to about −6.5 (Skinner et al., 2013), and thus 2 ε-units more radiogenic than today (−8.5; Goldstein & Hemming, 2003). In contrast, the glacial northern εNd end member is less well constrained due to lack of data. Thus, as a first approach, assuming a temporally constant northern εNd end member (−13.5, Goldstein & Hemming, 2003) for a binary mixing calculation, results in a 70% NCW contribution at CR during the LGM, which is in the range of 55–80% given by Howe, Piotrowski, Noble, et al. (2016). The assumption of a constant northern end member, however, may not be valid, as discussed in section 3.2. During the LGM a more unradiogenic northern end member is plausible, thus, setting the 70% NCW contribution calculated beforehand as an upper limit. A more extreme yet possible northern εNd end member of −20 for instance would yield a NCW contribution of about 40%.

A similar end member calculation can be performed for $\delta^{13}C$. For the LGM the northern end member is well constrained to be about 1.5‰ (Slowey & Curry, 1995). The southern end member is less certain but was assumed to be around −0.5‰ (Waelbroeck et al., 2011). This −0.5‰ estimate is from South Atlantic

10.1029/2017PA003290

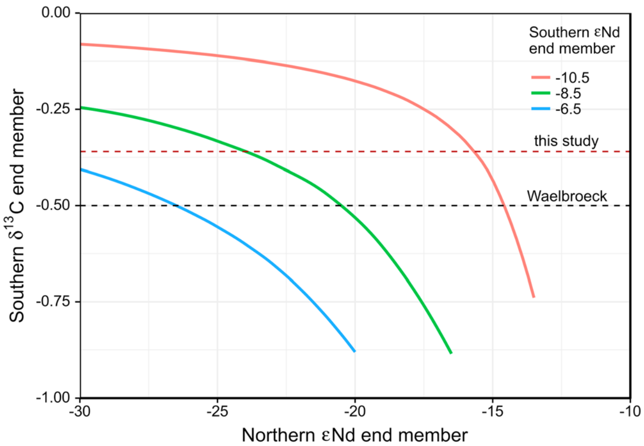

Figure 5. End member combinations of $\delta^{13}C$ and εNd that result in the same mixing proportion of northern and southern sourced water masses at Corner Rise during the Last Glacial Maximum, thus assuming quasi-conservative behavior of both proxies without decoupling. The northern $\delta^{13}C$ end member was fixed to 1.5‰ based on Slowey and Curry (1995). The southern εNd end member was varied from −6.5 (blue, proposed by Skinner et al., 2013), to −8.5 (green, modern value, Goldstein & Hemming, 2003) and −10.5 (red, HS1 value of Corner Rise, see text for explanation). Waelbroeck et al. (2011) estimated the southern $\delta^{13}C$ end member to be around −0.5‰ (black horizontal dashed line). New data from this study suggest a higher value of −0.36‰ (red horizontal dashed line). Under the assumption of conservative mixing, the equivalent northern εNd end member of the latter southern $\delta^{13}C$ end member and southern εNd end member of −6.5, −8.5, and −10.5 is <−30, −24, and −15.5, respectively.

cores mostly in the latitude band of 40°S to 50°S, and thus not necessarily representative of the Southern Ocean. In order to achieve an improved estimation we report stable isotope data on *Cibicidoides wuellerstorfi* from the LGM of core Atlantis II (AII) 107 22GGC, from the west flank of the Mid-Atlantic Ridge (54°48′S, 03°20′W, 2768 m water depth). The glacial interval of this core (Keigwin & Boyle, 1989) contains common *Cibicidoides wuellerstorfi*, and three measurements on two samples (67 and 69 cm) give $\delta^{13}C = -0.36 \pm 0.15$‰, and $\delta^{18}O = 4.39 \pm 0.23$‰. Although this LGM $\delta^{13}C$ value overlaps slightly with the value of Waelbroeck et al. (2011), it is also sufficiently greater than the CR value during HS1 that it suggests an aging effect of about ~0.1‰ on the northward flowing bottom water. The differences in the Dissolved Inorganic Carbon (DIC) concentrations are neglected here, since these differences between the southern and northern sourced end members are only in the order of 10% (Broecker & Peng, 1989) and are thus smaller than the uncertainties in the εNd calculation. The NCW contribution at CR calculated from these $\delta^{13}C$ end members (N: 1.5‰ and S: −0.36‰) is around 20–25% and is thus well below the upper limit (~70%) as well as the more extreme case (~40%) of the εNd calculation.

We therefore calculated possible end member combinations of the southern $\delta^{13}C$ and northern εNd end members yielding the same water mass mixing proportions (Figure 5), assuming conservative mixing for both proxies. The most realistic assumption for southern $\delta^{13}C$ and εNd end members is between −0.5‰ and −0.36‰ (Waelbroeck et al., 2011, and this study, respectively) and −6.5 (Skinner et al., 2013), respectively. The calculation of the corresponding northern εNd end member yields a value between −26 and <−30, which seems unrealistically low, even under the aspects discussed in section 3.2. While there are significant uncertainties in the southern $\delta^{13}C$ and northern εNd end members, these results thus indicate a decoupling between both water mass proxies.

However, one might argue that the signature recorded during HS1 at CR (−10.5) is the true value of southern sourced deep water entering the abyssal NW Atlantic basin after traveling from the Southern Ocean to about 35°N. This is based on the perception that NADW production was almost eliminated during HS1 (McManus et al., 2004), leading to pure SCW bathing the abyssal NW Atlantic. Thus, the Nd isotopic composition of deep SCW had to be modified from −6.5 in the Southern Ocean to −10.5 in the NW Atlantic either through mixing with shallower and less radiogenic Glacial North Atlantic Intermediate Water or nonconservative processes like boundary exchange or a benthic Nd flux (e.g., Haley et al., 2017; Jeandel, 2016) in the central and southern Atlantic. To calculate the binary mixing ratio of the deepest water masses at CR, this local southern εNd end member of −10.5 seems therefore more appropriate. Combining this new end member with a constant (i.e., modern) northern εNd end member yields a NCW contribution of about 30% at CR. The lower limit, however, is again even smaller, since the northern εNd end member was possibly also less radiogenic (see section 3.2).

Assuming conservative behavior of Nd isotopes and thus modification of the southern end member by water mass mixing during the transit through the Atlantic, the southern $\delta^{13}C$ end member should accordingly also be affected by the admixture of northern sourced shallow water to deep. Yet during HS1 the $\delta^{13}C$ value was −0.5‰ at CR and thus the same as the lower limit of the southern end member, indicating no admixture of northern sourced water. This contradicts the notion of conservative behavior of dissolved Nd and points again to a decoupling of both water mass proxies (Howe, Piotrowski, Noble, et al., 2016). These findings in combination with the uncertainties of the respective end members (and in case of Nd isotopes the unknown concentrations within paleo water masses) strongly limit the quantitative significance of mixing calculations. Yet although these calculations do not allow for an exact quantification of the exact water mass proportions, we can still infer from the $\delta^{13}C$ and εNd data that a nonzero proportion of northern sourced water contributed to the abyssal NW Atlantic during the LGM.

10.1029/2017PA003290

3.4. Water Mass Changes During the Deglaciation

The transition from HS1 to B/A at CR is characterized by an extremely sharp decrease in εNd of about 5 units, implying a rapid water mass change from SCW to NCW. This is consistent with a strengthened and/or deeper northern deep water production during the B/A (McManus et al., 2004; Thiagarajan et al., 2014). The εNd data from Bermuda Rise (Böhm et al., 2015; Gutjahr & Lippold, 2011; Roberts et al., 2010) corroborate this deep water mass change but with a smaller amplitude of only about $\Delta\varepsilon\mathrm{Nd} = -3$ (Figure 3). This discrepancy could imply either more unradiogenic material being transported to abyssal depth at the CR site (enhancing the pore water effect discussed in section 3.1) or a depth dependent and regionally variable NCW contribution. The latter infers that the strengthened deep water formation produced an unradiogenic bottom water that was mixed upward and diluted while propagating southward. Such an effect is further supported by the shallower cores IODP U1313 (3,428 m; Lippold et al., 2016, and this study) and SU90-03 (2,480 m; Howe, Piotrowski, & Rennie, 2016) that did not record such a B/A excursion (Figure 6).

Following the B/A, another water mass change was recorded at CR during the YD. A radiogenic excursion of $\Delta\varepsilon\mathrm{Nd} = +2.5$ indicates a return of increasing influence of southern sourced water and decreasing contributions from the Labrador Sea-derived signal. This increased contribution of southern water mass was present only for about 2 ka, in agreement with reduced northern deep water production during the YD (McManus et al., 2004). Again, similar to changes at the onset of the B/A, the YD event is also recorded in the Bermuda Rise data. Even though the change in amplitude is the same for both locations the Bermuda Rise data maintain their offset toward more radiogenic values, suggesting a consistently greater contribution of SCW at this shallower site and greater northern sourced contribution at the deeper site.

3.5. Implications of a Strong Holocene εNd Gradient

The Holocene AMOC circulation is thought to have been relatively stable compared to the changes of the deglaciation (Keigwin & Boyle, 2000). Recent findings of, for example, Howe, Piotrowski, and Rennie (2016), Lippold et al. (2016), and Roberts et al. (2010) show unexpected variations in records of NW Atlantic Nd isotopic composition of seawater for the early to mid-Holocene close to the 8.2-ka event (Alley et al., 1997). These unradiogenic excursions are either interpreted as enhanced LSW production (Lippold et al., 2016; Roberts et al., 2010) or as poorly chemically weathered detrital material deposited in the Labrador Sea as a pulse after Laurentide Ice Sheet retreat (Howe, Piotrowski, & Rennie, 2016).

While the timing of the 8.2-ka event matches the maximum of εNd variation in our record, we cannot directly link these two events with sufficient certainty since the age model is not well enough constrained during the Holocene (Figure 2). To explain the large amplitude of $\Delta\varepsilon\mathrm{Nd} = -9$ (compared to HS1) solely by a water mass change is unrealistic, because climatic variations during the early to mid-Holocene were smaller compared with the preceding deglacial major climate transitions and because it is unrealistic that the resulting εNd gradient between CR and Bermuda Rise is generated by water mass advection and mixing (Figure 3). Furthermore, a signal of $\varepsilon\mathrm{Nd} = -20$ is not achievable even with pure modern-like LSW (Lambelet et al., 2016). Thus, additional mechanisms, such as a pulse of detrital input described by Howe, Piotrowski, and Rennie (2016), must have played a significant role. Howe, Piotrowski, and Rennie (2016) suggested that this event produced an unradiogenic pulse propagating southward at abyssal depth. While attenuating through mixing with more radiogenic shallower water masses, such a process is capable to explain the offset between Bermuda Rise and the new CR εNd record. However, the stark Nd isotopic difference between the two sites during the early Holocene also suggests that such a process represents a strongly localized feature around the Labrador Sea (distance CR to Bermuda Rise: <460 nautical miles; Keigwin & Swift, 2017).

The gradual increase following this extreme excursion however indicates a rather smooth change in bottom water conditions which is thus not in agreement with a strong but singular unradiogenic pulse. Further, records from the whole NW Atlantic showing this gradual increase (Gutjahr et al., 2008; Lippold et al., 2016; Roberts et al., 2010) indicate a large-scale effect in contrast to the strongly localized pulse proposed by Howe, Piotrowski, and Rennie (2016), most likely related to postglacial chemical weathering and runoff effects in northeastern parts of North America bordering the NW Atlantic (cf. Kurzweil et al., 2010). Hence, the combination of two different processes may be responsible for the evolution of the εNd signatures of the local bottom water during the Holocene. In addition to the abovementioned localized process a

10.1029/2017PA003290

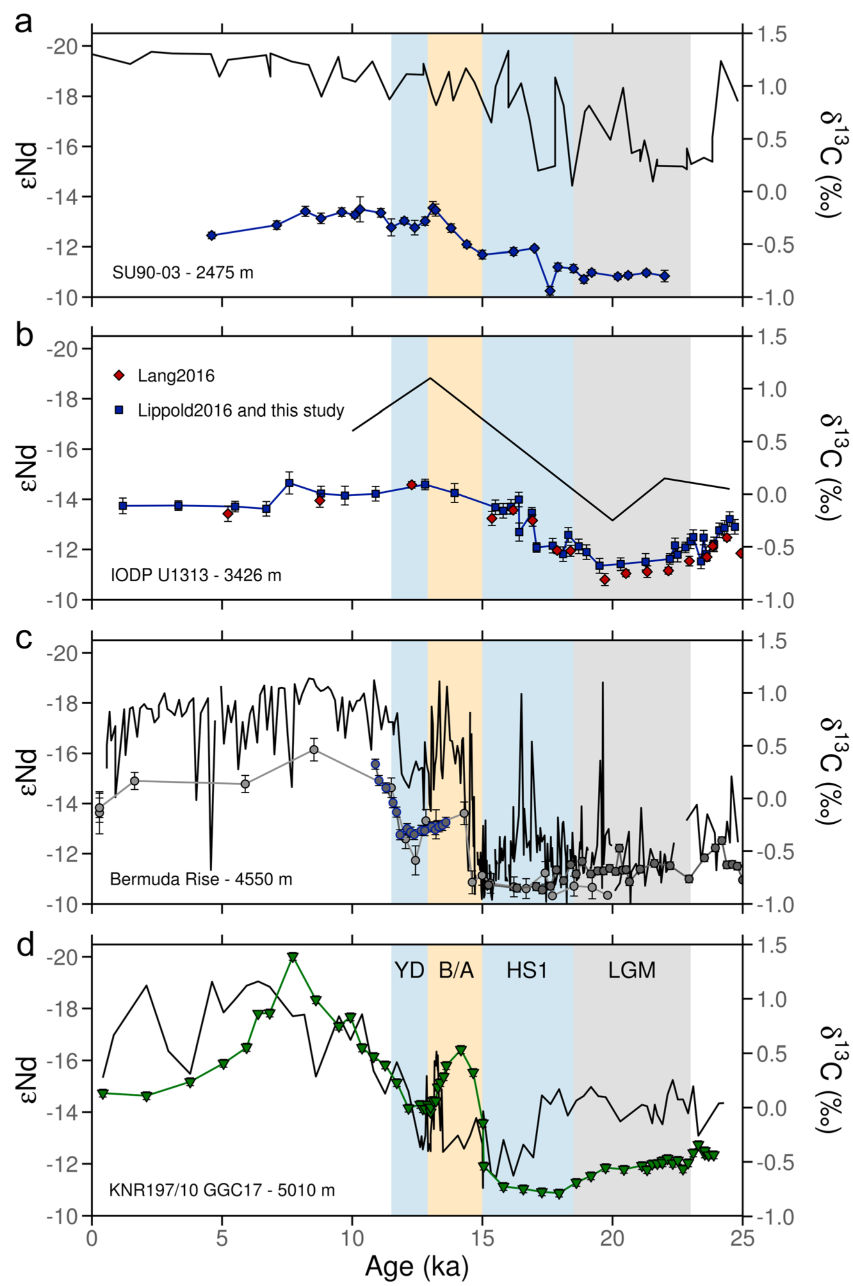

Figure 6. Comparison of εNd (filled symbols) and epibenthic $\delta^{13}C$ (black lines) from different NW Atlantic sites: (a) SU90-03 (Chapman & Shackleton, 1998; Howe, Piotrowski, & Rennie, 2016), (b) IODP U1313 (Lang et al., 2016; Lippold et al., 2016; Naafs et al., 2013; this study), (c) Bermuda Rise (Böhm et al., 2015; Gutjahr & Lippold, 2011; Keigwin & Boyle, 2000; Roberts et al., 2010), and (d) Corner Rise (this study; Keigwin & Swift, 2017). Note the reversed scales for εNd. Vertical bars indicate the time ranges of the LGM, HS1, B/A, and YD (same as Figures 2 and 3). LGM = Last Glacial Maximum; B/A = Bølling-Allerød; YD = Younger Dryas.

northern end member change that occurred most pronounced in the bottom water masses may be responsible for the less rapid changes. In this context, we note that Wilson et al. (2014) also proposed end member changes of intermediate northern sourced water. We speculate that such an end member change could have been realized by continuously decreasing contributions of reactive sediment by boundary exchange upstream the CR throughout the Holocene. In this scenario chemically poorly weathered detrital material deposited into the source regions of NWABW is buried underneath chemically more mature terrigenous material that was less reactive after deposition on the seafloor.

It is difficult to fully explain the Holocene variations in our εNd record from CR by one mechanism alone. We therefore propose an interplay of all three abovementioned processes of a water mass change, a detrital input into the Labrador Sea as described by Howe, Piotrowski, and Rennie (2016), and a gradual end member change of NWABW. While we are confident that the early Holocene shift after the YD toward less radiogenic signatures was dominated by the water mass change toward more NCW, the signal was most likely intensified by release of poorly chemically weathered detrital material (Howe, Piotrowski, & Rennie, 2016). It appears that the extreme excursion around 8 ka began at the end of the YD and culminated at the melt water pulse of the 8.2-ka event with the associated increased deposition of very unradiogenic poorly weathered detrital material (Alley et al., 1997; Howe, Piotrowski, & Rennie, 2016).The subsequent trend toward modern εNd values (from 7 to 2 ka) was either influenced by an end member change of NWABW or a successively decreasing contribution of reactive lithogenic material from the Labrador Sea within NWABW. Yet the resolvable εNd offset between core top and filtered seawater compositions today (see section 3.1) suggests that the process of reactive sediment deposition is still active today, albeit at significantly diminished magnitude. Future investigations upstream of the Labrador Sea may help to disentangle these processes affecting the Nd isotopic composition of lower NADW.

4. Conclusions

Neodymium isotopic data from the abyssal CR recorded several bottom water mass changes throughout the last 25 ka. Most obvious changes took place during the transitions from HS1 to B/A and from the YD to the Holocene, during which a “classical” displacement of SCW by NADW is observed (Gutjahr et al., 2008; Lippold et al., 2016; Piotrowski et al., 2005; Roberts et al., 2010; Sarnthein et al., 1994). The most extreme unradiogenic εNd signatures at the onset of the Holocene, however, were most likely influenced by a gradual end member change of NWABW and/or a pulse of poorly weathered detrital material (Howe, Piotrowski, & Rennie, 2016). The comparison of the CR data to the deglacial Bermuda Rise record (Roberts et al., 2010) reveals εNd and δ^{13}C changes, and thus most probable water mass changes, being most pronounced in the abyssal depth, attenuated upward.

In accordance with previous stable carbon isotope data (Keigwin & Swift, 2017) the Nd isotope record of CR suggests a distinct proportion of NCW contributing to the deepest water masses of the NW Atlantic during the LGM. A simple binary mixing model based on our new Nd isotopes data and the assumption of a fixed NCW εNd end member leads to an estimated NCW contribution to about 70%. This is in strong contrast to the 25% to 30% from the corresponding δ^{13}C end member calculation and indicates either potential εNd end member changes or partial decoupling and thus nonconservative behavior of one or both water mass proxies. Considering a likely Nd end member change and combining the end member calculations of δ^{13}C and εNd an estimated NCW contribution gives a lower limit of about 30%.

To reduce the uncertainty, the εNd end members of the deepest North and South Atlantic, the nonconservative impacts on εNd as well as the possible decoupling with δ^{13}C need to be better constrained. This would allow the exploration of the spatial extent of this NCW contribution in the abyssal NW Atlantic during the LGM.

Acknowledgments
We thank Ilse Glass and Laura Hauck for laboratory assistance as well as Scott Lehman for providing the ^{14}C AMS age of AII-107 22GGC. Sediment material was partly provided by the ODP/IODP core repository Bremen. Financial support for this research was provided by the Emmy-Noether Programme of the German Research Foundation (DFG) through grant Li1815/4. Figure was partly produced using the ODV software (Schlitzer, 2017. Ocean data view, http://odv.awi.de). Data from this study can be found in the supporting information (Tables S2–S5) and on Pangaea (www.pangaea.de). We further thank David Wilson and an anonymous reviewer for their detailed and constructive criticism.

References

Abbott, A. N., Haley, B. A., & McManus, J. (2016). The impact of sedimentary coatings on the diagenetic Nd flux. *Earth and Planetary Science Letters*, *449*, 217–227. https://doi.org/10.1016/j.epsl.2016.06.001

Adkins, J. F. (2013). The role of deep ocean circulation in setting glacial climates. *Paleoceanography*, *28*, 539–561. https://doi.org/10.1002/paleo.20046

Alley, R. B., Mayewski, P. A., Sowers, T., Stuiver, M., Taylor, K. C., & Clark, P. U. (1997). Holocene climatic instability: A prominent, widespread event 8200 yr ago. *Geology*, *25*(6), 483–486. https://doi.org/10.1130/0091-7613(1997)025%3C0483:HCIAPW%3E2.3.CO;2

Basak, C., Fröllje, H., Lamy, F., Gersonde, R., Benz, V., Anderson, R. F., et al. (2018). Breakup of last glacial deep stratification in the South Pacific. *Science*, *359*(6378), 900–904. https://doi.org/10.1126/science.aao2473

Biscaye, P. E., & Eittreim, S. L. (1977). Suspended particulate loads and transports in the nepheloid layer of the abyssal Atlantic Ocean. *Marine Geology*, *23*(1–2), 155–172. https://doi.org/10.1016/S0070-4571(08)70556-9

Blaser, P., Lippold, J., Gutjahr, M., Frank, N., Link, J. M., & Frank, M. (2016). Extracting foraminiferal Nd isotope signatures from bulk deep sea sediment by chemical leaching. *Chemical Geology*, *439*, 189–204. https://doi.org/10.1016/j.chemgeo.2016.06.024

Böhm, E., Lippold, J., Gutjahr, M., Frank, M., Blaser, P., Antz, B., et al. (2015). Strong and deep Atlantic Meridional Overturning Circulation during the last glacial cycle. *Nature*, *517*(7532), 73–76. https://doi.org/10.1038/nature14059

Boyle, E. A., & Keigwin, L. (1987). North Atlantic thermohaline circulation during the past 20,000 years linked to high-latitude surface temperature. *Nature*, *330*(6143), 35–40. https://doi.org/10.1038/330035a0

Bradtmiller, L. I., McManus, J. F., & Robinson, L. F. (2014). $^{231}Pa/^{230}Th$ evidence for a weakened but persistent Atlantic meridional overturning circulation during Heinrich Stadial 1. *Nature Communications*, *5*, 5817. https://doi.org/10.1038/ncomms6817

Broecker, W. S., & Peng, T.-H. (1989). The cause of the glacial to interglacial atmospheric CO_2 change: A polar alkalinity hypothesis. *Global Biogeochemical Cycles*, *3*(3), 215–239. https://doi.org/10.1029/GB003i003p00215

Chapman, M. R., & Shackleton, N. J. (1998). Millennial-scale fluctuations in North Atlantic heat flux during the last 150 000 years. *Earth and Planetary Science Letters*, *159*(1–2), 57–70. https://doi.org/10.1016/S0012-821X(98)00068-5

Cohen, A. S., O'Nions, R. K., Siegenthaler, R., & Griffin, W. L. (1988). Chronology of the pressure-temperature history recorded by a granulite terrain. *Contributions to Mineralogy and Petrology*, *98*(3), 303–311. https://doi.org/10.1007/BF00375181

Crocker, A. J., Chalk, T. B., Bailey, I., Spencer, M. R., Gutjahr, M., Foster, G. L., & Wilson, P. A. (2016). Geochemical response of the mid-depth Northeast Atlantic Ocean to freshwater input during Heinrich events 1 to 4. *Quaternary Science Reviews*, *151*, 236–254. https://doi.org/10.1016/j.quascirev.2016.08.035

Crocket, K. C., Vance, D., Gutjahr, M., Foster, G. L., & Richards, D. A. (2010). Persistent Nordic deep-overflow to the glacial North Atlantic. *Geology*, *39*(6), 515–518. https://doi.org/10.1130/G31677.1

Curry, W. B., & Oppo, D. W. (2005). Glacial water mass geometry and the distribution of $\delta^{13}C$ of CO_2 in the western Atlantic Ocean. *Paleoceanography*, *20*, PA1017. https://doi.org/10.1029/2004PA001021

Du, J., Haley, B. A., & Mix, A. C. (2016). Neodymium isotopes in authigenic phases, bottom waters and detrital sediments in the Gulf of Alaska and their implications for paleo-circulation reconstruction. *Geochimica et Cosmochimica Acta*, *193*, 14–35. https://doi.org/10.1016/j.gca.2016.08.005

Duplessy, J.-C., Moyes, J., & Pujol, C. (1980). Deep water formation in the North Atlantic Ocean during the last ice age. *Nature*, *286*(5772), 479–482. https://doi.org/10.1038/286479a0

Elmore, A. C., Wright, J. D., & Chalk, T. B. (2015). Precession-driven changes in Iceland-Scotland overflow water penetration and bottom water circulation on Gardar drift since ~200 ka. *Palaeogeography, Palaeoclimatology, Palaeoecology*, *440*, 551–563. https://doi.org/10.1016/j.palaeo.2015.09.042

Fagel, N., Hillaire-Marcel, C., & Robert, C. (1997). Changes in the Western Boundary Undercurrents Outflow since the Last Glacial Maximum, from smectite/illite ratios in deep Labrador Sea sediments. *Paleoceanography*, *12*(1), 79–96. https://doi.org/10.1029/96PA02877

Fagel, N., Innocent, C., Gariepy, C., & Hillaire-Marcel, C. (2002). Sources of Labrador Sea sediments since the Last Glacial Maximum inferred from Nd-Pb isotopes. *Geochimica et Cosmochimica Acta*, *66*(14), 2569–2581. https://doi.org/10.1016/S0016-7037(02)00866-9

Fagel, N., Innocent, C., Stevenson, R. K., & Hillaire-Marcel, C. (1999). Deep circulation changes in the Labrador Sea since the Last Glacial Maximum: New constraints from Sm-Nd data on sediments. *Paleoceanography*, *14*(6), 777–788. https://doi.org/10.1029/1999PA900041

Frank, M. (2002). Radiogenic isotopes: Tracers of past ocean circulation and erosional input. *Reviews of Geophysics*, *40*(1), 1001. https://doi.org/10.1029/2000RG000094

Garcia, H. E., Locarnini, R. A., Boyer, T. P., Antonov, J. I., Baranova, O. K., Zweng, M. M., et al. (2014). World Ocean Atlas 2013, volume 4: Dissolved inorganic nutrients (phosphate, nitrate, silicate). In S. Levitus & A. Mishonov (Eds.), *NOAA Atlas NESDIS 76* (25 pp.).

Gebbie, G. (2014). How much did glacial North Atlantic water shoal? *Paleoceanography*, *29*, 190–209. https://doi.org/10.1002/2013PA002557

Gebbie, G., Peterson, C. D., Lisiecki, L. E., & Spero, H. J. (2015). Global-mean marine $\delta^{13}C$ and its uncertainty in a glacial state estimate. *Quaternary Science Reviews*, *125*, 144–159. https://doi.org/10.1016/j.quascirev.2015.08.010

Goldstein, S. L., & Hemming, S. R. (2003). Long-lived isotopic tracers in oceanography, paleoceanography, and ice-sheet dynamics. *Treatise on Geochemistry*, *6*, 453–489. https://doi.org/10.1016/B0-08-043751-6/06179-X

Grützner, J., Gison, L., Franz, S. O., Tiedemann, R., Cortijo, E., Chaisson, W. P., et al. (2002). Astronomical age models for Pleistocene drift sediments from the western North Atlantic (ODP Sites 1055–1063). *Marine Geology*, *189*(1-2), 5–23. https://doi.org/10.1016/S0025-3227(02)00320-1

Gutjahr, M., Frank, M., Stirling, C. H., Keigwin, L. D., & Halliday, A. N. (2008). Tracing the Nd isotope evolution of North Atlantic deep and intermediate waters in the western North Atlantic since the Last Glacial Maximum from Blake Ridge sediments. *Earth and Planetary Science Letters*, *266*(1–2), 61–77. https://doi.org/10.1016/j.epsl.2007.10.037

Gutjahr, M., Frank, M., Stirling, C. H., Klemm, V., van de Flierdt, T., & Halliday, A. N. (2007). Reliable extraction of a deepwater trace metal isotope signal from Fe-Mn oxyhydroxide coatings of marine sediments. *Chemical Geology*, *242*(3–4), 351–370. https://doi.org/10.1016/j.chemgeo.2007.03.021

Gutjahr, M., & Lippold, J. (2011). Early arrival of southern source water in the deep North Atlantic prior to Heinrich event 2. *Paleoceanography*, *26*, PA2101. https://doi.org/10.1029/2011PA002114

Haley, B. A., Du, J., Abbott, A. N., & McManus, J. (2017). The impact of benthic processes on rare Earth element and neodymium isotope distributions in the oceans. *Frontiers in Marine Science*, *4*, 1–12. https://doi.org/10.3389/fmars.2017.00426

Haley, B. A., Klinkhammer, G. P., & McManus, J. F. (2004). Rare Earth elements in pore waters of marine sediments. *Geochimica et Cosmochimica Acta*, *68*(6), 1265–1279. https://doi.org/10.1016/j.gca.2003.09.012

Howe, J. N. W., Piotrowski, A. M., Noble, T. L., Mulitza, S., Chiessi, C. M., & Bayon, G. (2016). North Atlantic deep water production during the Last Glacial Maximum. *Nature Communications*, *7*, 11765. https://doi.org/10.1038/ncomms11765

Howe, J. N. W., Piotrowski, A. M., & Rennie, V. C. F. (2016). Abyssal origin for the early Holocene pulse of unradiogenic neodymium isotopes in Atlantic seawater. *Geology*, *44*, 831–834. https://doi.org/10.1130/G38155.1

Jeandel, C. (2016). Overview of the mechanisms that could explain the 'boundary exchange' at the land–ocean contact. *Philosophical Transactions of the Royal Society A*, *374*(2081), 20150287. https://doi.org/10.1098/rsta.2015.0287

Jeandel, C., Arsouze, T., Lacan, F., Téchiné, P., & Dutay, J.-C. (2007). Isotopic Nd compositions and concentrations of the lithogenic inputs into the ocean: A compilation, with an emphasis on the margins. *Chemical Geology*, *239*(1–2), 156–164. https://doi.org/10.1016/j.chemgeo.2006.11.013

Keigwin, L. D. (2004). Radiocarbon and stable isotope constraints on Last Glacial Maximum and Younger Dryas ventilation in the western North Atlantic. *Paleoceanography*, *19*, PA2001. https://doi.org/10.1029/2004PA001029

Keigwin, L. D., & Boyle, E. A. (1989). Late Quaternary paleochemistry of high-latitude surface waters. *Palaeogeography, Palaeoclimatology, Palaeoecology*, *73*(1-2), 85–106. https://doi.org/10.1016/0031-0182(89)90047-3

Keigwin, L. D., & Boyle, E. A. (2000). Detecting Holocene changes in thermohaline circulation. *Proceedings of the National Academy of Sciences of the United States of America*, *97*(4), 1343–1346. https://doi.org/10.1073/pnas.97.4.1343

Keigwin, L. D., & Boyle, E. A. (2008). Did North Atlantic overturning halt 17,000 years ago? *Paleoceanography*, *23*, PA1101. https://doi.org/10.1029/2007PA001500

Keigwin, L. D., & Swift, S. A. (2017). Carbon isotope evidence for a northern source of deep water in the glacial western North Atlantic. *Proceedings of the National Academy of Sciences of the United States of America*, *114*(11), 2831–2835. https://doi.org/10.1073/pnas.1614693114

Kurzweil, F., Gutjahr, M., Vance, D., & Keigwin, L. D. (2010). Authigenic Pb isotopes from the Laurentian Fan: Changes in chemical weathering and patterns of North American freshwater runoff during the last deglaciation. *Earth and Planetary Science Letters*, *299*(3–4), 458–465. https://doi.org/10.1016/j.epsl.2010.09.031

Lacan, F., & Jeandel, C. (2004). Denmark Strait water circulation traced by heterogeneity in neodymium isotopic composition. *Deep Sea Research, Part I*, *51*(1), 71–82. https://doi.org/10.1016/j.dsr.2003.09.006

Lacan, F., & Jeandel, C. (2005a). Neodymium isotopes as a new tool for quantifying exchange fluxes at the continent-ocean interface. *Earth and Planetary Science Letters*, *232*(3–4), 245–257. https://doi.org/10.1016/j.epsl.2005.01.004

Lacan, F., & Jeandel, C. (2005b). Acquisition of the neodymium isotopic composition of the North Atlantic Deep Water. *Geochemistry, Geophysics, Geosystems*, *6*, Q12008. https://doi.org/10.1029/2005GC000956

Lacan, F., Tachikawa, K., & Jeandel, C. (2012). Neodymium isotopic composition of the oceans: A compilation of seawater data. *Chemical Geology*, *300-301*, 177–184. https://doi.org/10.1016/j.chemgeo.2012.01.019

Lambelet, M., van de Flierdt, T., Crocket, K., Rehkämper, M., Kreissig, K., Coles, B., et al. (2016). Neodymium isotopic composition and concentration in the western North Atlantic Ocean: Results from the GEOTRACES GA02 section. *Geochimica et Cosmochimica Acta*, *177*, 1–29. https://doi.org/10.1016/j.gca.2015.12.019

Lang, D. C., Bailey, I., Wilson, P. A., Chalk, T. B., Foster, G. L., & Gutjahr, M. (2016). Incursions of southern-sourced water into the deep North Atlantic during Late Pliocene Glacial Intensification. *Nature Geoscience*, *9*(5), 375–379. https://doi.org/10.1038/ngeo2688

Lippold, J., Grützner, J., Winter, D., Lahaye, Y., Mangini, A., & Christl, M. (2009). Does sedimentary ^{231}Pa/^{230}Th from the Bermuda rise monitor past Atlantic meridional overturning circulation? *Geophysical Research Letters*, *36*, L12601. https://doi.org/10.1029/2009GL038068

Lippold, J., Gutjahr, M., Blaser, P., Christner, E., de Carvalho Ferreira, M. L., Mulitza, S., & Jaccard, S. L. (2016). Deep water provenience and dynamics of the (de)glacial Atlantic meridional overturning circulation. *Earth and Planetary Science Letters*, *445*, 68–78. https://doi.org/10.1016/j.epsl.2016.04.013

McManus, J. F., Francois, R., Gherardi, J.-M., Keigwin, L. D., & Brown-Leger, S. (2004). Collapse and rapid resumption of Atlantic meridional circulation linked to deglacial climate changes. *Nature*, *428*(6985), 834–837. https://doi.org/10.1038/nature02494

Middag, R., van Hulten, M. M. P., Van Aken, H. M., Rijkenberg, M. J. A., Gerringa, L. J. A., Laan, P., & de Baar, H. J. W. (2015). Dissolved aluminium in the ocean conveyer of the West Atlantic Ocean: Effects of the biological cycle, scavenging, sediment resuspension and hydrography. *Marine Chemistry*, *177*, 69–86. https://doi.org/10.1016/j.marchem.2015.02.015

Millo, C., Sarnthein, M., Voelker, A., & Erlenkeuser, H. (2006). Variability of the Denmark Strait overflow during the Last Glacial Maximum. *Boreas*, *35*(1), 50–60. https://doi.org/10.1080/03009480500359244

Naafs, B. D. A., Hefter, J., Grützner, J., & Stein, R. (2013). Warming of surface waters in the mid-latitude North Atlantic during Heinrich events. *Paleoceanography*, *28*, 153–163. https://doi.org/10.1029/2012PA002354

NGRIP Members (2004). High-resolution record of Northern Hemisphere climate extending into the last interglacial period. *Nature*, *431*(7005), 147–151. https://doi.org/10.1038/nature02805

Palmer, M. R. (1985). Rare Earth elements in foraminifera tests. *Earth and Planetary Science Letters*, *73*(2–4), 285–298. https://doi.org/10.1016/0012-821X(85)90077-9

Piepgras, D. J., & Wasserburg, G. J. (1987). Rare Earth element transport in the western North Atlantic inferred from Nd isotopic observations. *Geochimica et Cosmochimica Acta*, *51*(5), 1257–1271. https://doi.org/10.1016/0016-7037(87)90217-1

Pin, C., Briot, D., Bassin, C., & Poitrasson, F. (1994). Concomitant separation of strontium and samarium-neodymium for isotopic analysis in silicate samples, based on specific extraction chromatography. *Analytica Chimica Acta*, *298*(2), 209–217. https://doi.org/10.1016/0003-2670(94)00274-6

Piotrowski, A. M., Galy, A., Nicholl, J. A. L., Roberts, N., Wilson, D. J., Clegg, J. A., & Yu, J. (2012). Reconstructing deglacial North and South Atlantic deep water sourcing using foraminiferal Nd isotopes. *Earth and Planetary Science Letters*, *357-358*, 289–297. https://doi.org/10.1016/j.epsl.2012.09.036

Piotrowski, A. M., Goldstein, S. L., Hemming, S. R., & Fairbanks, R. G. (2005). Temporal relationships of carbon cycling and ocean circulation at glacial boundaries. *Science*, *307*(5717), 1933–1938. https://doi.org/10.1126/science.1104883

Piotrowski, A. M., Goldstein, S. L., Hemming, S. R., Fairbanks, R. G., & Zylberberg, D. R. (2008). Oscillating glacial northern and southern deep water formation from combined neodymium and carbon isotopes. *Earth and Planetary Science Letters*, *272*, 394–405. https://doi.org/10.1016/j.epsl.2008.05.011

Rempfer, J., Stocker, T. F., Joos, F., Dutay, J.-C., & Siddall, M. (2011). Modelling Nd-isotopes with a coarse resolution ocean circulation model: Sensitivities to model parameters and source/sink distributions. *Geochimica et Cosmochimica Acta*, *75*(20), 5927–5950. https://doi.org/10.1016/j.gca.2011.07.044

Rijkenberg, M. J. A., Middag, R., Laan, P., Gerringa, L. J. A., Van Aken, H. M., De Jong, J. T. M., & De Baar, H. J. W. (2014). The distribution of dissolved iron in the West Atlantic Ocean. *PLoS One*, *9*(6), e101323–e101314. https://doi.org/10.1371/journal.pone.0101323

Roberts, N. L., Piotrowski, A. M., McManus, J. F., & Keigwin, L. D. (2010). Synchronous deglacial overturning and water mass source changes. *Science*, *327*(5961), 75–78. https://doi.org/10.1126/science.1178068

Sarnthein, M., Winn, K., Jung, S. J. A., Duplessy, J.-C., Labeyrie, L., Erlenkeuser, H., & Ganssen, G. (1994). Changes in East Atlantic Deepwater Circulation over the last 30,000 years: Eight time slice reconstructions. *Paleoceanography*, *9*(2), 209–267. https://doi.org/10.1029/93PA03301

Schlitzer, R. (2017). Ocean Data View. Retrieved from odv.awi.de

Schmitz, W. J. (1996). On the world ocean circulation: Volume I some global features/North Atlantic circulation. *Woods Hole Oceanographic Institution Technical Report, WHOI-96-03*. doi:https://doi.org/10.1575/1912/355

Skinner, L. C., Scrivner, A. E., Vance, D., Barker, S., Fallon, S., & Waelbroeck, C. (2013). North Atlantic versus Southern Ocean contribution to a deglacial surge in deep ocean ventilation. *Geology*, *41*(6), 667–670. https://doi.org/10.1130/G34133.1

Slowey, N. C., & Curry, W. B. (1995). Glacial-interglacial differences in circulation and carbon cycling within the upper western North Atlantic. *Paleoceanography*, *10*(4), 715–732. https://doi.org/10.1029/95PA01166

Stichel, T., Frank, M., Rickli, J., & Haley, B. A. (2012). The hafnium and neodymium isotope composition of seawater in the Atlantic sector of the Southern Ocean. *Earth and Planetary Science Letters*, *317-318*, 282–294. https://doi.org/10.1016/j.epsl.2011.11.025

Tachikawa, K., Athias, V., & Jeandel, C. (2003). Neodymium budget in the modern ocean and paleo-oceanographic implications. *Journal of Geophysical Research*, *108*(C8), 3254. https://doi.org/10.1029/1999JC000285

Tanaka, T., Togashi, S., Kamioka, H., Amakawa, H., Kagami, H., Hamamoto, T., et al. (2000). JNdi-1: A neodymium isotopic reference in consistency with LaJolla neodymium. *Chemical Geology*, *168*(3–4), 279–281. https://doi.org/10.1016/S0009-2541(00)00198-4

Thiagarajan, N., Subhas, A. V., Southon, J. R., Eiler, J. M., & Adkins, J. F. (2014). Abrupt pre-Bølling-Allerød warming and circulation changes in the deep ocean. *Nature*, *511*(7507), 75–78. https://doi.org/10.1038/nature13472

Thornalley, D. J. R., Bauch, H. A., Gebbie, G., Guo, W., Ziegler, M., Bernasconi, S. M., et al. (2015). A warm and poorly ventilated deep Arctic Mediterranean during the last glacial period. *Science*, *349*(6249), 706–710. https://doi.org/10.1126/science.aaa9554
van de Flierdt, T., Griffiths, A. M., Lambelet, M., Little, S. H., Stichel, T., & Wilson, D. J. (2016). Neodymium in the oceans: A global database, a regional comparison and implications for paleoceanographic research. *Philosophical Transactions of the Royal Society A*, *374*(2081), 20150293. https://doi.org/10.1098/rsta.2015.0293
van de Flierdt, T., Robinson, L. F., & Adkins, J. F. (2010). Deep-sea coral aragonite as a recorder for the neodymium isotopic composition of seawater. *Geochimica et Cosmochimica Acta*, *74*(21), 6014–6032. https://doi.org/10.1016/j.gca.2010.08.001
Vance, D., Scrivner, A. E., Beney, P., Staubwasser, M., Henderson, G. M., & Slowey, N. C. (2004). The use of foraminifera as a record of the past neodymium isotope composition of seawater. *Paleoceanography*, *19*, PA2009. https://doi.org/10.1029/2003PA000957
Waelbroeck, C., Skinner, L. C., Labeyrie, L., Duplessy, J. C., Michel, E., Vazquez Riveiros, N., et al. (2011). The timing of deglacial circulation changes in the Atlantic. *Paleoceanography*, *26*, PA3213. https://doi.org/10.1029/2010PA002007
Wilson, D. J., Crocket, K. C., van de Flierdt, T., Robinson, L. F., & Adkins, J. F. (2014). Dynamic intermediate ocean circulation in the North Atlantic during Heinrich Stadial 1: A radiocarbon and neodymium isotope perspective. *Paleoceanography*, *29*, 1072–1093. https://doi.org/10.1002/2014PA002674
Wilson, D. J., Piotrowski, A. M., Galy, A., & Clegg, J. A. (2013). Reactivity of neodymium carriers in deep sea sediments: Implications for boundary exchange and paleoceanography. *Geochimica et Cosmochimica Acta*, *109*, 197–221. https://doi.org/10.1016/j.gca.2013.01.042